

Density, Viscosity, and Performances of Carbon Dioxide Capture in 16 Absorbents of Amine + Ionic Liquid + H₂O, Ionic Liquid + H₂O, and Amine + H₂O Systems

Yansong Zhao,^{†,‡} Xiangping Zhang,^{*,†} Shaojuan Zeng,[†] Qing Zhou,[†] Haifeng Dong,^{†,‡} Xiao Tian,^{†,‡} and Suojiang Zhang[†]

State Key Laboratory of Multiphase Complex System, Institute of Process Engineering, Chinese Academy of Sciences, Beijing 100190, People's Republic of China, and College of Chemistry and Chemical Engineering, Graduate University of Chinese Academy of Sciences, Beijing 100049, People's Republic of China

A series of novel ionic liquids, 2-aminoethanol tetrafluoroborate ([MEA][BF₄]), 2-[2-hydroxyethyl(methyl)amino] ethanol tetrafluoroborate ([MDEA][BF₄]), 2-[2-hydroxyethyl(methyl)amino] ethanol chloride ([MDEA][Cl]), 2-[2-hydroxyethyl(methyl)amino] ethanol phosphate ([MDEA][PO₄]), and 2-[2-hydroxyethyl(methyl)amino] ethanol sulfate ([MDEA][SO₄]), were synthesized and characterized for carbon dioxide capture in this work. Densities and viscosities of ionic liquids (1-butyl-3-methylimidazolium tetrafluoroborate, [MEB][BF₄], [MDEA][BF₄], [MDEA][Cl], [MDEA][PO₄], and [MDEA][SO₄]), amines + ionic liquids + H₂O, ionic liquids + H₂O, and amines + H₂O were measured at temperatures ranging from (303.15 to 343.15) K at different mass fractions. These 16 different absorbents were prepared by mixing two or three compounds of 2-aminoethanol (MEA), 2-[2-hydroxyethyl(methyl)amino] ethanol (MDEA), 2-[bis(2-hydroxyethyl)amino] ethanol (TEA), ionic liquids, and water. The carbon dioxide capture rate and carbon dioxide capture capacity in the 16 different absorbents were measured at 303.15 K and 1.50 MPa. The experimental results showed that the viscosities of these absorbents are less than 17.00 mPa·s at 303.15 K. Among these absorbents, the MDEA + [MDEA][Cl] + H₂O + piperazine system shows the best performance on carbon dioxide capture.

Introduction

With the deterioration of climate change in recent years, as a main source of CO₂ emissions, fossil fuel will remain the world's dominant source of energy for a long period of time. To reverse this trend, technologies that can help to reduce CO₂ emissions from fossil fuels are taken into consideration. CO₂ capture and storage (CCS) is particularly promising.¹ Thus, many hotspots have been focused on how to explore a high efficiency and environment-friendly capture technology with lower energy consumption compared with the current used technologies. At present, chemical absorption is an effective way to separate CO₂ from industrial gases,^{2–6} such as oil recovery gases, nature gases,⁷ syngas, and so on. The typical solvent is an amine, including 2-aminoethanol (MEA), 2-[2-hydroxyethyl(methyl)amino] ethanol (MDEA), 2-(2-hydroxyethylamino)ethanol (DEA), and 2-[bis(2-hydroxyethyl)amino] ethanol (TEA), or mixtures of amines as the common absorbents to capture CO₂.^{8–11} However, in light of their corrosion, volatility, toxicity, and high energy consumption, in recent years, some ionic liquids (ILs), such as 1-butyl-3-methylimidazolium tetrafluoroborate ([Bmim][BF₄]), 1-butyl-3-methylimidazolium hexafluorophosphate ([Bmim][PF₆]), tetrabutylphosphonium amino acid ILs ([P(C₄)₄][AA]),¹² and hydroxyl ammonium ILs¹³ are designed and synthesized as absorbents to absorb and separate CO₂ from the mixture gases.^{7,14–20} ILs manifest the excellent properties of recycling, being contamination-free,

functionality, and high efficiency of scrubbing CO₂; thus, the IL-based capture process appears probably to be the promising choice of alternative or competitive technologies.

Although ILs, including functionalized and conventional ILs, have shown their inspiring prospects for CO₂ capture,²¹ the industrialization or commercialization still faces some bottlenecks due to their high viscosity, high price, and so on. Recently researchers have reported that composite absorbents (mixture of amines and ILs) could perform well in CO₂ capture and may lead a bright future of CO₂ capture industrialization.²² However, using traditional ILs, such as [Bmim][BF₄], [Bmim][Cl], and so on, still can not resolve the high price problem and improve the CO₂ capacity apparently because the low solubility of CO₂ in these ILs. In this work, novel task-specific ILs, 2-aminoethanol tetrafluoroborate ([MEA][BF₄]), 2-[2-hydroxyethyl(methyl)amino] ethanol tetrafluoroborate ([MDEA][BF₄]), 2-[2-hydroxyethyl(methyl)amino] ethanol chloride ([MDEA][Cl]), 2-[2-hydroxyethyl(methyl)amino] ethanol phosphate ([MDEA][PO₄]), and 2-[2-hydroxyethyl(methyl)amino] ethanol sulfate ([MDEA][SO₄]) are synthesized according to our previous patent.²³ This study mainly focuses on the physical properties and CO₂ capture performances of 16 composite absorbents.

Experimental Section

Materials. The chemicals used in this work were obtained from Beijing Chemical Works and Henan Lihua Pharmaceutical Co., Ltd. ([hmim][Tf₂N] was synthesized in our laboratory). The mass fraction purities of [Bmim][BF₄] (CAS R.N. 174501-65-6), [hmim][Tf₂N] (CAS R.N. 382150-50-7), MEA (CAS R.N. 9007-33-4), TEA (CAS R.N. 7376-31-0), and MDEA (CAS

* Corresponding author. Tel.: +86 10 62558174. Fax: +86 10 82627080. E-mail address: xpzhang@home.ipe.ac.cn (Xiangping Zhang).

[†] Institute of Process Engineering, Chinese Academy of Sciences.

[‡] Graduate University of Chinese Academy of Sciences.

Scheme 1. Synthesis of ILs: R and R': H, -CH₃, or -CH₂-CH₂-OH; B: BF₄⁻, Cl⁻, SO₄²⁻, or PO₄³⁻; n: 1, 2, or 3

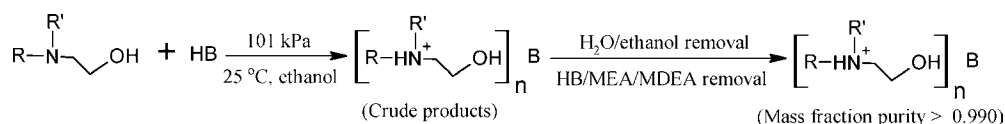


Table 1. Density (ρ) and Viscosity (η) of Pure 2-[2-Hydroxyethyl(methyl)amino] Ethanol (MDEA) from $T = (303.15 \text{ to } 343.15) \text{ K}$

T/K	$\rho/\text{g}\cdot\text{cm}^{-3}$		$\eta/\text{mPa}\cdot\text{s}$	
	this work	lit.	this work	lit.
303.15	1.033738	1.0337 ²⁵	57.69	57.57 ²⁵
313.15	1.026719	1.0267 ²⁵	34.79	34.78 ²⁵
323.15	1.019481	1.0194 ²⁵	21.88	21.98 ²⁵
333.15	1.012322	1.0123 ²⁵	14.60	14.5 ²⁵
343.15	1.002249	1.00183 ²⁶	9.855	9.850 ²⁶

R.N. 511262-76-3) were ≥ 0.990 , which were checked by gas chromatography (Agilent 7890, Agilent Technologies Inc., U.S.) or high-performance liquid chromatography (Agilent 1100, Agilent Technologies Inc., U.S.) before use. Hydrochloric acid (HCl + H₂O) (CAS R.N. 7647-01-0, $0.36 \leq w \leq 0.38$), fluoboric acid (HBF₄ + H₂O) (CAS R.N. 13814-97-6, $w \geq 0.40$), sulfuric acid (H₂SO₄ + H₂O) (CAS R.N. 7664-93-9, $w \geq 0.98$), and phosphoric acid (H₃PO₄ + H₂O) (CAS R.N. 7664-38-2, $w \geq 0.85$) were also used in this work (w , mass fraction purity).

Synthesis of ILs. ILs of [MEA][BF₄], [MDEA][BF₄], [MDEA][Cl], [MDEA][SO₄], and [MDEA][PO₄] were synthesized in our laboratory by a neutralization reaction. The synthesis process of ILs was shown in Scheme 1. For instance, to obtain [MDEA][Cl] the synthesis procedure was introduced as follows: 9.5947 g of HCl and 11.9160 g of MDEA were accurately weighed. HCl was put into a drip funnel, and then it was dripped into a three-necked flask filled with MDEA; 20 mL of ethanol was added into the flask as the reaction solvent. The reaction was carried out stirring by a magnetic stirrer for 12 h at 298.15 K and 101 kPa. After that, most of the H₂O and ethanol in the mixture were removed by distillation at the proper temperature and pressure. Then, the raw product was purified by extraction using acetone to remove the remaining HCl or MDEA. Finally, the product was put into a vacuum oven to get the final ILs [MDEA][Cl]. The other four ILs [MEA][BF₄], [MDEA][BF₄], [MDEA][SO₄], and [MDEA][PO₄], were also prepared by a similar method, respectively. They were dried in a vacuum oven for 72 h, and the water content was tested by a moisture analyzer (787 KF Titrino, Metrohm, Switzerland) to confirm that the water mass fraction was $< 5 \cdot 10^{-5}$.

Characterization of ILs. The purities of ILs were checked by high-performance liquid chromatography or a Fourier transform infrared (FTIR) instrument (WS-NEXUS670IR, Nicolet, U.S.). The infrared spectra of ILs were tested at 400 cm⁻¹ to 4000 cm⁻¹ by the FTIR instrument with ILs filled in the microsample holder. The samples of ILs were also characterized by the ¹H NMR spectrum (600 MHz), using D₂O or CDCl₃ as solvent with tetramethylsilane as an internal standard.

Absorbents Preparation. All absorbents were weighed by an electronic analytical balance (BS124S, Sartorius Scientific Instrument Co. Ltd., China) with precision of $\pm 0.0001 \text{ g}$. Absorbents of TEA + H₂O, TEA + [Bmim][BF₄], TEA + [Bmim][BF₄] + H₂O, MEA + H₂O, MDEA + H₂O, [Bmim][BF₄] + H₂O, [MEA][BF₄] + H₂O, [MDEA][BF₄] + H₂O, [MDEA][Cl] + H₂O, [MDEA][PO₄] + H₂O, [MDEA][SO₄] + H₂O, MEA + [MEA][BF₄] + H₂O, MDEA + [MDEA][Cl] + H₂O, MDEA + [MDEA][PO₄] + H₂O, MDEA + [MDEA][SO₄] + H₂O, and MDEA + [MDEA][Cl] + H₂O + piperazine (PZ) in certain mass fractions were prepared before experiments. Especially, the binary mixture TEA + [Bmim][BF₄] with different TEA mass fractions, 0.0000, 0.1998, 0.3987, 0.5005, 0.7999, and 1.0000, respectively, was also prepared for further research.

Density. Densities of the absorbents and ILs were measured by a density meter (Anton Paar DMA 5000, Anton Paar Co., Austria). The temperature of this study was between (303.15 and 343.15) K, at 10 K intervals, the precision of which was $\pm 0.001 \text{ K}$ (the temperature accuracy is controlled traceably to national standards by two integrated Pt 100 platinum thermometers), and the absolute room pressure was approximately 101 kPa at that time. The repeatability of every piece of density data was $\pm 0.000001 \text{ g}\cdot\text{cm}^{-3}$, and the accuracy of density measurements was $\pm 0.000005 \text{ g}\cdot\text{cm}^{-3}$, which was calibrated with ultrapure water and dry air. The same data point of the same sample with one injection into the apparatus was measured five times, and the average of the data was calculated as the final density. The overall average relative error density measurement²⁴ for MDEA, [Bmim][BF₄], and [hmim][Tf₂N] is less than 0.0115 %, 0.3187 %, and 0.2139 % (calculated by eq 1), respectively, according to the data from Tables 1 and 2.

Table 2. Density (ρ) and Viscosity (η) of Pure 1-Butyl-3-methylimidazolium Tetrafluoroborate ([Bmim][BF₄]) and 1-Hexyl-3-methylimidazolium Bis(trifluoromethyl)sulfonyl Amide ([hmim][Tf₂N]) from $T = (303.15 \text{ to } 343.15) \text{ K}$

T/K	$\rho/\text{g}\cdot\text{cm}^{-3}$		$\eta/\text{mPa}\cdot\text{s}$	
	this work	lit.	this work	lit.
	[Bmim][BF ₄]			
303.15	1.195698	1.2005 \pm 0.025, ²⁷ 1.1984 ²⁸	68.90	80.7, ¹⁸ 74.21, ²⁸ 233, ³⁰ 56 \pm 0.8 ³¹
313.15	1.188618	1.1940 \pm 0.0014, ²⁷ 1.1922 ²⁸	44.73	51.3, ¹⁸ 46.51, ²⁸ 37.1 \pm 0.7 ³¹
323.15	1.181591	1.1860 ²⁷	30.81	34.6, ¹⁸ 31.08 ²⁸
333.15	1.174603	1.1747 \pm 0.0001, ²⁹ 1.1798 ²⁸	22.28	24.5, ¹⁸ 21.52 ²⁸
343.15	1.167672	1.1737 \pm 0.0022, ²⁷ 1.1647 ²⁸	16.75	18.1, ¹⁸ 15.61 ²⁸
	[hmim][Tf ₂ N]			
303.15	1.364542	1.3674 ³²	56.63	57 ³³
313.15	1.355433	1.3583 ³²	37.74	37.7 ³³
323.15	1.346365	1.3493 ³²	26.56	
333.15	1.337352	1.3402 ³²	19.52	19.5 ³³
343.15	1.328278	1.3312 ³²	14.93	14.9 ³³

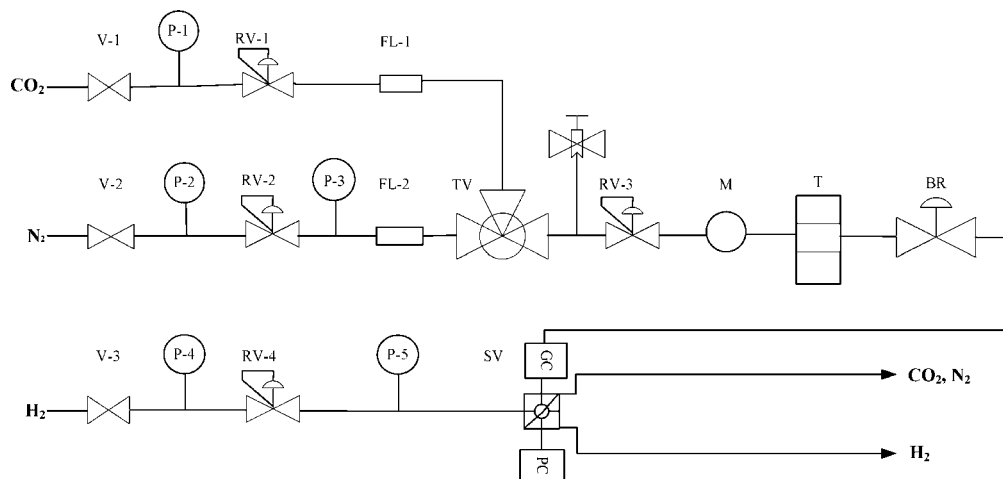


Figure 1. Flow sheet of CO₂ capture experimental apparatus: BR, back pressure regulator; FL, gas flow meter; GC, gas chromatography; M, mixer; P, pressure gauge; PC, computer; RV, regulating valve; SV, six-way valve; T, CO₂ capture tower; TV, three-way valve; V, stop valve.

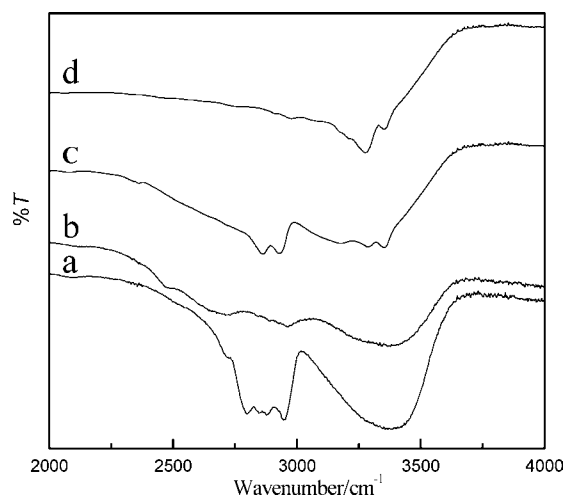


Figure 2. IR spectra of MDEA, [MDEA][BF₄], MEA, and [MEA][BF₄]: a, MDEA; b, [MDEA][BF₄]; c, MEA; d, [MEA][BF₄].

Viscosity. Viscosities of absorbents and ILs were measured by a viscosity meter (Anton Paar AMVn, Anton Paar Co., Austria) with a reproducibility < 0.5 % and repeatability < 0.1 %, and calibration was carried out using ultrapure water or viscosity standard oils (No. H117, Anton Paar Co., Austria). The temperature range of this study was from (303.15 to 343.15) K, at 10 K intervals, the precision of which was ± 0.01 K (the temperature accuracy is controlled by a built-in precise Peltier thermostat), and the absolute room pressure was approximate

101 kPa at that time. The overall average relative error viscosity measurement²⁴ for MDEA, [Bmim][BF₄], and [hmim][Tf₂N] is less than 0.2865 %, 4.537 %, and 0.2648 % (calculated by eq 1), respectively, according to the data from Tables 1 and 2.

Apparatus and Procedure of CO₂ Capture. The CO₂ capture rate and capacity in the absorbents were measured by the experimental apparatus shown in Figure 1. CO₂ capture rate and capacity in the 16 absorbents were tested at 303.15 K and 1.50 MPa (total pressure), with a precision of ± 0.1 K and 0.1 %, respectively. In the experimental procedure, the volume flow of N₂ and CO₂ was 300 mL·min⁻¹ and 100 mL·min⁻¹ controlled by gas flow meters (D07-11A/ZM, Beijing Sevenstar Electronics Co., Ltd., China). They were mixed together in the mixer (M as shown in Figure 1); CO₂ of the mixture gas was captured by absorbents in capture tower (T as shown in Figure 1). The concentration of CO₂ was measured by gas chromatography online. The CO₂ capture rate will be obtained from the concentration–time curves of CO₂ (N₂ capture capacity in absorbents is much lower than that of CO₂; it is reasonable to consider the volume flow of N₂ is constant IN and OUT the capture tower). Finally, the CO₂ capture capacity could be obtained. The capture process lasted for (8 to 9) h to achieve the absorption saturation; 525.00 mL of absorbent was used at every experiment.

Results and Discussion

Characterization of ILs. Structures of ILs [MEA][BF₄], [MDEA][BF₄], [MDEA][PO₄], and [MDEA][Cl] could be

Table 3. Density (ρ) and Viscosity (η) of TEA (1) + [Bmim][BF₄] (2) at Different TEA Mass Fractions from $T = (303.15 \text{ to } 343.15) \text{ K}$ (w_1 , Mass Fraction)

T/K	w_1						
	0.0000	0.1998	0.3987	0.5005	0.6000	0.7999	1.0000
	$\rho/\text{g}\cdot\text{cm}^{-3}$						
303.15	1.195698	1.175802	1.161098	1.150075	1.146422	1.129558	1.114431
313.15	1.188618	1.168629	1.154409	1.142895	1.139614	1.123215	1.108343
323.15	1.181591	1.161503	1.146935	1.135481	1.132761	1.116727	1.102230
333.15	1.174603	1.154441	1.139884	1.128119	1.125887	1.110165	1.095962
343.15	1.167672	1.147422	1.132867	1.120990	1.119000	1.103538	1.089599
	$\eta/\text{mPa}\cdot\text{s}$						
303.15	68.90	57.94	69.54	86.62	116.5	186.3	398.2
313.15	44.73	35.89	39.71	47.22	60.67	99.43	195.9
323.15	30.81	24.02	25.08	28.82	36.10	54.02	103.6
333.15	22.28	17.13	17.08	19.11	23.35	33.63	60.81
343.15	16.75	12.82	12.32	13.48	16.14	22.33	37.94

Table 4. Density (ρ) and Viscosity (η) of Pure ILs from $T = (303.15 \text{ to } 343.15) \text{ K}$

T/K	ILs				
	[MEA][BF ₄]	[MDEA][BF ₄]	[MDEA][SO ₄]	[MDEA][PO ₄]	[MDEA][Cl]
	$\rho/\text{g}\cdot\text{cm}^{-3}$				
303.15	1.490568	1.425560	1.282487	1.215952	1.180417
313.15	1.482624	1.418100	1.276834	1.208495	1.174706
323.15	1.474942	1.410628	1.271249	1.200877	1.169237
333.15	1.467845	1.403199	1.265719	1.193226	1.163747
343.15	1.464590	1.395851	1.260243	1.185523	1.158285
	$\eta/\text{mPa}\cdot\text{s}$				
303.15	59.39	208.8			512.1
313.15	48.68	117.7	1858	2483	278.2
323.15	33.96	71.79	990.8	1426	164.2
333.15	32.85	46.85	571.2	822.5	104.1
343.15	27.84	32.35	350.4	385.4	70.45

Table 5. Density (ρ) and Viscosity (η) of Amines (1) + H₂O (2) from $T = (303.15 \text{ to } 343.15) \text{ K}$ (w , Mass Fraction)

T/K	$\rho/\text{g}\cdot\text{cm}^{-3}$			$\eta/\text{mPa}\cdot\text{s}$		
	$w_1 = 0.3000$	$w_1 = 0.3002$	$w_1 = 0.3002$	$w_1 = 0.3000$	$w_1 = 0.3002$	$w_1 = 0.3002$
	TEA + H ₂ O	MEA + H ₂ O	MDEA + H ₂ O	TEA + H ₂ O	MEA + H ₂ O	MDEA + H ₂ O
303.15	1.042753	1.013021	1.022898	2.354	2.093	2.612
313.15	1.037935	1.007984	1.018001	1.799	1.603	1.937
323.15	1.032207	1.003422	1.012963	1.425	1.271	1.505
333.15	1.023739	0.997157	1.006922	1.172	1.037	1.207
343.15	1.011676	0.989924	0.992641	0.9591	0.8681	0.8944

Table 6. Density (ρ) and Viscosity (η) of Amines (1) + ILs (2) + H₂O (3) from $T = (303.15 \text{ to } 343.15) \text{ K}$ (w , Mass Fraction)

T/K	$w_1 = 0.3000$	$w_1 = 0.3006$	$w_1 = 0.3001$	$w_1 = 0.3000$	$w_1 = 0.3000$	$w_1 = 0.2999$
	$w_2 = 0.3001$	$w_2 = 0.2996$	$w_2 = 0.3002$	$w_2 = 0.3001$	$w_2 = 0.3001$	$w_2 = 0.3003$ $w_3 = 0.3499$
	TEA + [Bmim][BF ₄] + H ₂ O	MEA + [MEA][BF ₄] + H ₂ O	MDEA + [MDEA][Cl] + H ₂ O	MDEA + [MDEA][PO ₄] + H ₂ O	MDEA + [MDEA][SO ₄] + H ₂ O	MDEA + [MDEA][Cl] + H ₂ O + PZ
	$\rho/\text{g}\cdot\text{cm}^{-3}$					
303.15	1.096023	1.180501	1.081634	1.098871	1.116498	1.083504
313.15	1.089288	1.173199	1.075645	1.092118	1.110182	1.077210
323.15	1.082119	1.165895	1.069476	1.085150	1.103660	1.070740
333.15	1.074877	1.158851	1.063089	1.077926	1.097050	1.064117
343.15	1.065953	1.151905	1.056515	1.070424	1.090266	1.057292
	$\eta/\text{mPa}\cdot\text{s}$					
303.15	1.245	6.442	7.601	16.99	11.67	12.78
313.15	1.041	4.785	5.424	10.08	8.039	8.813
323.15	0.8831	3.718	3.997	6.957	5.831	6.362
333.15	0.7874	2.998	3.061	5.021	4.387	4.759
343.15	0.7196	2.469	2.410	3.762	3.404	3.689

Table 7. Density (ρ) and Viscosity (η) of ILs (1) + H₂O (2) from $T = (303.15 \text{ to } 343.15) \text{ K}$ (w , Mass Fraction)

T/K	$w_1 = 0.2998$	$w_1 = 0.3004$	$w_1 = 0.3001$	$w_1 = 0.3006$	$w_1 = 0.3007$	$w_1 = 0.2999$
	[Bmim][BF ₄] + H ₂ O	[MEA][BF ₄] + H ₂ O	[MDEA][BF ₄] + H ₂ O	[MDEA][Cl] + H ₂ O	[MDEA][PO ₄] + H ₂ O	[MDEA][SO ₄] + H ₂ O
	$\rho/\text{g}\cdot\text{cm}^{-3}$					
303.15	1.045351	1.116484	1.084708	1.058437	1.075319	1.091950
313.15	1.039844	1.110851	1.075109	1.053895	1.070311	1.087460
323.15	1.033761	1.104951	1.067019	1.049230	1.063440	1.082240
333.15	1.027742	1.098991	1.058010	1.043307	1.055386	1.075886
343.15	1.021176	1.093412	1.047871	1.037052	1.045379	1.068318
	$\eta/\text{mPa}\cdot\text{s}$					
303.15	1.292	1.007	1.245	1.539	2.630	1.795
313.15	1.046	0.8573	1.041	1.265	2.125	1.446
323.15	0.8731	0.7412	0.8831	1.067	1.805	1.196
333.15	0.7473	0.6743	0.7874	0.8862	1.594	1.012
343.15	0.6549	0.5896	0.7196	0.7911	1.455	0.8720

definitely confirmed by ¹H NMR and FTIR. For example, we could get the structures of the MEA, [MEA][BF₄], MDEA, and [MDEA][Cl] from the ¹H NMR characterization results. ¹H NMR (600 MHz, D₂O) of MEA: 3.43 (t, 2H), 2.57 (t, 2H); ¹H NMR (600 MHz, D₂O) of [MEA][BF₄]: 3.44 (t, 2H), 2.57 (t, 2H); ¹H NMR (600 MHz, DMSO-*d*₆) of MDEA: 4.31 (s, 2H), 3.44 (t, 4H), 2.41 (t, 4H), 2.19 (s, 3H); ¹H NMR

(600 MHz, DMSO-*d*₆) of [MDEA][Cl]: 4.43 (s, 2H), 3.57 (t, 4H), 2.81 (t, 4H), 2.27 (s, 3H). It was showed that the hydroxyl functional group of MEA and MDEA was not destroyed in the neutralization reaction as the characteristic peak of hydroxyl functional group could be seen at approximately 3400 cm⁻¹ from the FTIR spectra shown in Figure 2.

Table 8. Parameters of Equation 2 and AADs for Density Correlation of TEA (1) + [Bmim][BF₄] (2) (w, Mass Fraction)

w_1	A_0	$10^4 A_1$	$10^7 A_2$	100 AAD
0.0000	1.4332	-8.5624	2.4071	0.0204
0.1998	1.4185	-8.8121	2.6571	0.0179
0.3987	1.3591	-6.0231	-1.6643	0.0232
0.5005	1.3827	-8.0055	1.1000	0.0086
0.6000	1.3410	-6.0308	-1.2786	0.0084
0.7999	1.2792	-3.5453	-4.5857	0.0304
1.0000	1.2501	-2.9499	-5.0357	0.0341

Table 9. Parameters of Equation 3 and AADs for Viscosity Correlation of TEA (1) + [Bmim][BF₄] (2) (w, Mass Fraction)

w_1	A_0	A_1	A_2	100 AAD
0.0000	-1.6034	729.8667	-178.0884	0.0266
0.1998	-1.2527	535.3853	-202.3660	0.1180
0.3987	-1.5400	540.2290	-209.7122	0.2455
0.5005	-1.5067	527.7116	-214.7297	0.1227
0.6000	-1.3287	508.5156	-219.6015	0.7632
0.7999	-5.2199	1598.9143	-150.1196	8.0964
1.0000	-3.2458	1090.9065	-185.0076	9.5573

Density and Viscosity. We compared the density and viscosity of pure MDEA and [Bmim][BF₄] obtained from our experiments with the data from literature to check the accuracy of the measured density and viscosity, which was listed in Tables 1 and 2. The densities and viscosities of pure MDEA in this work are in good agreement with that in the work of Al-Ghawar et al.²⁵ and Henni et al.,²⁶ as was shown in Table 1. Meanwhile, densities of pure [Bmim][BF₄] in this work were also in agreement with that in the work of Van Valkenburg et al., Zhou et al., and Fredlake et al.^{27–29} However, viscosities of pure [Bmim][BF₄] in current literature did not agree with each other quite well: 80.7 mPa·s at 303.15 K in ref 18, 233 mPa·s at 303.15 K in ref 30, and (56 ± 0.8) mPa·s at 303.15 K in ref 31, but in this work the value is 68.08 mPa·s at 303.15 K, which is between that of in ref 18 and ref 31. The results show that our experimental data are in good agreement with previous literature, especially with ref 28. Especially, density and viscosity of [hmim][Tf₂N] were listed in Table 2 to check the accuracy of the experimental apparatus according to the reviewer's suggestion. It was shown that the density and viscosity of pure [hmim][Tf₂N] in this work were in good agreement with that in the work of Marsh et al.³² and Goodwin et al.,³³ which illustrated that the value of density and viscosity in this work was dependable. The density and viscosity of absorbents and ILs were listed in Tables 3 to 7. The measured data of densities and viscosities listed in Tables 1 to 7 could be fitted and regressed by the equations as follows:²

$$\text{ADD} = \frac{1}{n} \sum_{i=1}^n |\rho_{i,\text{exptl}} - \rho_{i,\text{calcd}}| \quad (1)$$

$$\rho/\text{g}\cdot\text{cm}^{-3} = A_0 + A_1(T/\text{K}) + A_2(T/\text{K})^2 \quad (2)$$

$$\mu/\text{mPa}\cdot\text{s} = \exp\left[A_0 + \frac{A_1}{T/\text{K} + A_2}\right] \quad (3)$$

where ρ and η stood for the densities and the viscosities, A_0 , A_1 , and A_2 were the quadratic fitting regression parameters with the least-squares method, and ADD was the average absolute deviation between the experimental results and the calculated values by eqs 2 and 3. For instance, the densities and viscosities of TEA + [Bmim][BF₄] were fitted by eqs 2 and 3, and the values of A_0 , A_1 , A_2 , and ADD were listed in Tables 8 and 9. The tendency of the densities and viscosities changing with temperature was shown in Figures 3 and 4. Densities and viscosities changing with temperature in other absorbents could also be fitted with a similar tendency.

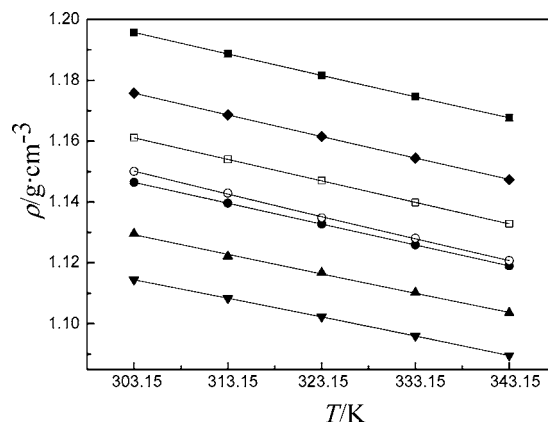


Figure 3. Density of TEA + [Bmim][BF₄] as a function of temperature at different TEA mass fractions: ■, 0.0000; ◆, 0.1998; □, 0.3987; ○, 0.5005; ●, 0.6000; ▲, 0.7999; ▼, 1.0000. The symbols represent experimental values, and the solid curves represent the values calculated from eq 2.

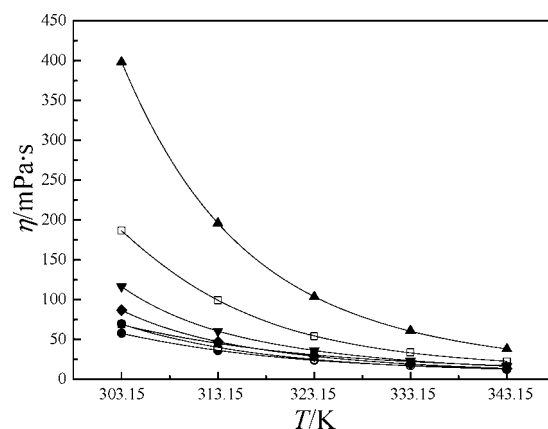


Figure 4. Viscosity of TEA + [Bmim][BF₄] as a function of temperature at different TEA mass fractions: ●, 0.0000; ○, 0.1998; ■, 0.3987; ◆, 0.5005; ▼, 0.6000; □, 0.7999; ▲, 1.0000. The symbols represent experimental values, and the solid curves represent the values calculated from eq 3.

Performances of CO₂ Capture. The CO₂ capture capacity was listed in Table 10, with an uncertainty of ± 2.5 % (calculated by error transferring method). The repeatability of CO₂ capture capacity is ± 0.5 % according to the data of the three times measurements for the same sample. We checked our measurement of MDEA + H₂O with the work of Jou et al.³⁴ and Kuranov et al.,³⁵ and the measurement was in agreement with the literature value (relative deviation < 1.6 %).

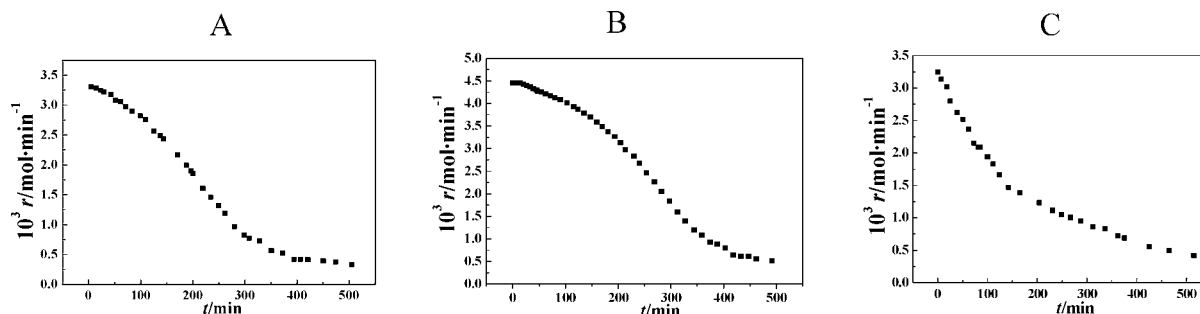


Figure 5. CO₂ capture rate in different absorbents at different times: A, TEA + H₂O; B, TEA + [Bmim][BF₄] + H₂O; C, TEA + [Bmim][BF₄]. The symbols represent CO₂ capture rate values.

Table 10. CO₂ Capture Capacity (g CO₂/g absorbent) in Various Capture Systems, Amines (1) + ILs (2) + H₂O (3), ILs (2) + H₂O (3), and Amines (1) + H₂O (3) at 303.15 K and 1.50 MPa (Total Pressure) (*w*, Mass Fraction)

absorbents	<i>w</i> ₁	<i>w</i> ₂	<i>w</i> ₃	CO ₂ capture capacity
TEA + [Bmim][BF ₄]	0.3001	0.6999		0.121
TEA + [Bmim][BF ₄] + H ₂ O	0.3000	0.3001	0.3999	0.166
TEA + H ₂ O	0.3000		0.7000	0.129
MEA + H ₂ O	0.3002		0.6998	0.159
MDEA + H ₂ O	0.3002		0.6998	0.130
[Bmim][BF ₄] + H ₂ O		0.2998	0.7002	0.021
[MEA][BF ₄] + H ₂ O		0.3004	0.6996	0.028
[MDEA][BF ₄] + H ₂ O		0.3001	0.6999	0.085
[MDEA][Cl] + H ₂ O		0.3006	0.6994	0.028
[MDEA][PO ₄] + H ₂ O		0.3007	0.6993	0.067
[MDEA][SO ₄] + H ₂ O		0.2999	0.7001	0.054
MEA + [MEA][BF ₄] + H ₂ O	0.3006	0.2996	0.3998	0.167
MDEA + [MDEA][Cl] + H ₂ O	0.3001	0.3002	0.3997	0.142
MDEA + [MDEA][PO ₄] + H ₂ O	0.3000	0.3001	0.3999	0.132
MDEA + [MDEA][SO ₄] + H ₂ O	0.3000	0.3001	0.3999	0.135
MDEA + [MDEA][Cl] + H ₂ O + PZ	0.2999 + 0.0499 (MDEA + PZ)	0.3003	0.3499	0.158

For absorbents of TEA (1) + H₂O (2) (*w*₁ = 0.3000), TEA (1) + [Bmim][BF₄] (2) + H₂O (3) (*w*₁ = 0.3000, *w*₂ = 0.3001), and TEA (1) + [Bmim][BF₄] (2) (*w*₁ = 0.3001), the CO₂ capture rate of them was shown in Figure 5 according to concentration–time curves of CO₂. Then, the CO₂ capture capacity could be calculated. From Table 10, it was shown that CO₂ capture capacity of TEA + [Bmim][BF₄] + H₂O was larger than that of TEA + H₂O and TEA + [Bmim][BF₄].

However, solvent losses of MDEA are smaller than that of MEA and TEA.³⁵ Therefore, composite absorbents with MDEA were investigated especially in this work. It was shown that 1.000 g of absorbent of MDEA + [MDEA][Cl] + H₂O could capture 0.142 g of CO₂. To improve the capture rate and capacity of this absorbent, PZ was added into it as an activator.³⁶ It was shown that 1.000 g of MDEA + [MDEA][Cl] + H₂O + PZ could capture 0.158 g of CO₂ after the addition of PZ. The CO₂ capture rate and capacity in this absorbent did not decrease after four times capture and regeneration work.

Conclusion

In this work densities, viscosities, and the CO₂ capture rate and capacity of 16 various absorbents were measured. Because of the existence of ILs, the composite absorbents have a better performance in CO₂ capture, and the viscosities are also lower than that of current ILs. Besides, energy consumption in the regeneration of these absorbents is less than that of current traditional amine absorbents. It is shown that 1.000 g of absorbent of MDEA + [MDEA][Cl] + H₂O + PZ could capture 0.158 g of CO₂, which illustrates that IL absorbents have a

significant potential application prospect for CO₂ capture; therefore, further study will focus on this system.

Literature Cited

- (1) Damen, K.; Faaij, A.; Turkenburg, W. Pathways towards large-scale implementation of CO₂ capture and storage: a case study for the Netherlands. *Int. J. Greenhouse Gas Control* **2009**, *3*, 217–236.
- (2) Choi, L. S.; Lee, S. M.; Maken, S.; Song, H. J.; Shin, H. C.; Park, J. W.; Jang, K. R.; Kim, J. H. Physical properties of aqueous sodium glycinate solution as an absorbent for carbon dioxide removal. *J. Chem. Eng. Data* **2005**, *50*, 1773–1776.
- (3) Zhang, Y. Q.; Zhang, S. J.; Lu, X. M.; Zhou, Q.; Fan, W.; Zhang, X. P. Dual amino-functionalised phosphonium ionic liquids for CO₂ capture. *Chem.—Eur. J.* **2009**, *15*, 3003–3011.
- (4) Haszeldine, R. S. Carbon capture and storage: how green can black be. *Science* **2009**, *325*, 1647–1652.
- (5) Rochelle, G. T. Amine scrubbing for CO₂ capture. *Science* **2009**, *325*, 1652–1654.
- (6) Bara, J. E.; Carlisle, T. K.; Gabriel, C. J.; Camper, D.; Finotello, A.; Gin, D. L.; Noble, R. D. Guide to CO₂ separations in imidazolium-based room-temperature ionic liquids. *Ind. Eng. Chem. Res.* **2009**, *48*, 2739–2751.
- (7) Galán Sánchez, L. M.; Meindersma, G. W.; De Haan, A. B. Solvent properties of functionalized ionic liquids for CO₂ absorption. *Chem. Eng. Res. Des.* **2007**, *85*, 31–39.
- (8) Lin, S. H.; Chiang, P. C.; Hsieh, C. F.; Li, M. H.; Tung, K. L. Absorption of carbon dioxide by the absorbent composed of piperazine and 2-amino-2-methyl-1-propanol in PVDF membrane contactor. *J. Chin. Inst. Chem. Eng.* **2008**, *39*, 13–21.
- (9) Park, S. W.; Choi, B. S.; Oh, K. J.; Lee, J. W. Absorption of carbon dioxide into aqueous PAA solution containing diethanolamine. *J. Chin. Inst. Chem. Eng.* **2007**, *38*, 461–466.
- (10) Boucif, N.; Favre, E.; Roizard, D. CO₂ capture in HFMM contactor with typical amine solutions: a numerical analysis. *Chem. Eng. Sci.* **2008**, *63*, 5375–5385.
- (11) Bishno, S.; Rochel, G. T. Absorption of carbon dioxide in aqueous piperazine/methyldiethanolamine. *AIChE J.* **2002**, *48*, 2788–2799.
- (12) Zhang, J. M.; Zhang, S. J.; Dong, K.; Zhang, Y. Q.; Shen, Y. Q. Supported absorption of CO₂ by tetrabutylphosphonium amino acid ionic liquids. *Chem.—Eur. J.* **2006**, *12*, 4021–4026.

- (13) Yuan, X. L.; Zhang, S. J.; Liu, J.; Lu, X. M. Solubility of CO₂ in hydroxyl ammonium ionic liquids at elevated pressures. *Fluid Phase Equilib.* **2007**, *257*, 195–200.
- (14) Sarraute, S.; Gomes, G. M. C.; Païdua, A. A. H. Diffusion coefficients of 1-alkyl-3-methylimidazolium ionic liquids in water, methanol and acetonitrile at infinite dilution. *J. Chem. Eng. Data* **2009**, *54*, 2389–2394.
- (15) Kumelan, J.; Tuma, D.; Kamps, A. P.; Maurer, G. Solubility of the single gases carbon dioxide and hydrogen in the ionic liquid [bmpy][Tf₂N]. *J. Chem. Eng. Data* **2010**, *55*, 165–172.
- (16) Muldoon, M. J.; Anderson, J. L.; Dixon, J. K.; Brennecke, J. F. Improving carbon dioxide solubility in ionic liquids. *J. Phys. Chem.* **2007**, *111*, 9001–9009.
- (17) Hebach, A.; Oberhof, A.; Dahmen, N.; Griesheimer, P. Interfacial tension of two ionic liquids, 1-ethyl-3-methylimidazolium 2-(2-ethoxyethoxy) ethylsulfate and 1-butyl-3-methylimidazolium 2-(2-methoxyethoxy)ethylsulfate, with compressed CO₂. *J. Chem. Eng. Data* **2009**, *54*, 1249–1253.
- (18) Chang, H. C.; Jiang, J. C.; Chang, C. Y.; Su, J. C.; Hung, C. H.; Liou, Y. C.; Lin, S. H. Structural organization in aqueous solutions of 1-butyl-3-methylimidazolium halides: a high-pressure infrared spectroscopic study on ionic liquids. *J. Phys. Chem. B* **2008**, *112*, 4351–4356.
- (19) Borodin, O.; Smith, G. D. Structure and dynamics of *N*-methyl-*N*-propylpyrrolidinium bis(trifluoromethanesulfonyl)imide ionic liquid from molecular dynamics simulations. *J. Phys. Chem. B* **2006**, *110*, 11481–11490.
- (20) Harris, K. R.; Kanakubo, M.; Woolf, L. A. Temperature and pressure dependence of the viscosity of the ionic liquid 1-butyl-3-methylimidazolium tetrafluoroborate: viscosity and density relationships in ionic liquids. *J. Chem. Eng. Data* **2007**, *52*, 2425–2430.
- (21) Bates, E. D.; Mayton, R. D.; Ntai, L.; Davis, J. H. CO₂ capture by a task-specific ionic liquid. *J. Am. Chem. Soc.* **2002**, *124*, 926–927.
- (22) Camper, D.; Bara, J. E.; Gin, D. L.; Noble, R. D. Room-temperature ionic liquid-amine solutions: tunable solvents for efficient and reversible capture of CO₂. *Ind. Eng. Chem. Res.* **2008**, *47*, 8496–8498.
- (23) Zhang, X. P.; Zhao, Y. S.; Zeng, S. J.; Zhang, S. J.; Liu, L.; Tian, X. Synthesis of a task-specific alcamine ionic liquids. CN Patent 200910093071.X, 2009.
- (24) Fan, W.; Zhou, Q.; Sun, J.; Zhang, S. J. Density, Excess molar volume, and viscosity for the methyl methacrylate + 1-butyl-3-methylimidazolium hexafluorophosphate ionic liquid binary system at atmospheric pressure. *J. Chem. Eng. Data* **2009**, *54*, 2307–2311.
- (25) Al-Ghawas, H. A.; Hagewlesche, D. P.; Rulz-Ibanez, G.; Sandal, O. C. Physicochemical properties important for carbon dioxide absorption in aqueous methyl-diethanolamine. *J. Chem. Eng. Data* **1989**, *34*, 385–391.
- (26) Henni, A.; Maham, Y.; Tontiwachwuthikul, P.; Chakma, A.; Mather, A. E. Densities and viscosities for binary mixtures of *N*-methyl-diethanolamine + triethylene glycol monomethyl ether from 25 °C to 70 °C and *N*-methyl-diethanolamine + ethanol mixtures at 40 °C. *J. Chem. Eng. Data* **2000**, *45*, 247–253.
- (27) Fredlake, C. P.; Hert, D. G.; Brennecke, J. F. Thermophysical properties of imidazolium-based ionic liquids. *J. Chem. Eng. Data* **2004**, *49*, 954–964.
- (28) Zhou, Q.; Wang, L. S.; Chen, H. P. Densities and viscosities of 1-butyl-3-methylimidazolium tetrafluoroborate + H₂O binary mixtures from (303.15 to 353.15) K. *J. Chem. Eng. Data* **2006**, *51*, 905–908.
- (29) Van Valkenburg, M. E.; Williams, M.; Wilkes, J. S. Thermochemistry of ionic liquid heat-transfer fluids. *Thermochim. Acta* **2005**, *425*, 181–188.
- (30) Deng, M. J.; Chen, P. Y.; Leong, T. I.; Sun, I. W.; Chang, J. K.; Tsai, W. T. Dicyanamide anion based ionic liquids for electrodeposition of metals. *Electrochem. Commun.* **2008**, *10*, 213–216.
- (31) Qia, M.; Wua, G.; Lic, Q.; Luoc, Y. r-Radiation effect on ionic liquid [Bmim][BF₄]. *Radiat. Phys. Chem.* **2008**, *77*, 877–883.
- (32) Marsh, K. N.; Brennecke, J. F.; Chirico, R. D.; Frenkel, M.; Heintz, A.; Magee, J. W.; Peters, C. J.; Rebelo, L. P. N.; Seddon, K. R. Thermodynamic and thermophysical properties of the reference ionic liquid: 1-hexyl-3-methylimidazolium bis[(trifluoromethyl)sulfonyl]amide. *Pure Appl. Chem.* **2009**, *81*, 781–790.
- (33) Kandil, M. E.; Marsh, K. N.; Goodwin, A. R. H. Measurement of the viscosity, density, and electrical conductivity of 1-hexyl-3-methylimidazolium bis(trifluorosulfonyl)imide at temperatures between (288 and 433) K and pressures below 50 MPa. *J. Chem. Eng. Data* **2007**, *52*, 2382–2387.
- (34) Jou, F.; Mather, A. E.; Otto, F. D. Solubility of H₂S and CO₂ in aqueous methyl-diethanolamine solutions. *Ind. Eng. Chem. Process Des. Dev.* **1982**, *21*, 539–544.
- (35) Kuranov, G.; Rumpf, R.; Smirnova, N. A.; Maurer, G. Solubility of single gases carbon dioxide and hydrogen sulfide in aqueous solutions of *N*-methyl-diethanolamine in the temperature range 313–413 K at pressures up to 5 MPa. *Ind. Eng. Chem. Res.* **1996**, *35*, 1959–1966.
- (36) Speyer, D.; Ermatchkov, V.; Maurer, G. Solubility of carbon dioxide in aqueous solutions of *N*-methyl-diethanolamine and piperazine in the low gas loading region. *J. Chem. Eng. Data* **2010**, *55*, 283–290.

Received for review February 21, 2010. Accepted June 15, 2010. The authors sincerely appreciate National Natural Science Funds for Distinguished Young Scholar (No. 20625618), National Natural Science Foundation of China (Grant No. 20806083), and Knowledge Innovation Program of the Chinese Academy of Sciences (No. KG CX2-YW-321) for the financial support.

JE100078W